The Gallium Anomaly

M.Sc. Thesis

By

Harshit Joshi

DEPARTMENT OF PHYSICS

INDIAN INSTITUTE OF TECHNOLOGY

INDORE

JUNE 2024

The Gallium Anomaly

A THESIS

Submitted in partial fulfillment of the requirements for the award of the degree of

Master of Science

by

Harshit Joshi

(Roll No.2203151030)

Under the guidance of

Prof. Subhendu Rakshit

DEPARTMENT OF PHYSICS

INDIAN INSTITUTE OF TECHNOLOGY INDORE

JUNE 2024

INDIAN INSTITUTE OF TECHNOLOGY INDORE

CANDIDATE'S DECLARATION

I hereby certify that the work which is being presented in the thesis entitled **"The Gallium Anomaly"** in the partial fulfillment of the requirements for the award of the degree of **MASTER OF SCIENCE** and submitted in the **DEPARTMENT OF PHYSICS**, **Indian Institute of Technology Indore**, is an authentic record of my own work carried out during the time period from July 2023 to June 2024 under the supervision of **Prof. Subhendu Rakshit**, Department of Physics, IIT Indore. The matter presented in this thesis by me has not been submitted for the award of any other degree of this or any other institute.

Harshit Joshi

Signature of the student

(**Harshit Joshi**)

This is to certify that the above statement made by the candidate is correct to the best of my knowledge.

Subhendu Rakshit

Signature of Thesis Supervisor

(**Prof. Subhendu Rakshit**)

Harshit Joshi has successfully given his M.Sc. Oral Examination held on 15th May, 2024.

Subhendu Rakshit

Signature of supervisor of M.Sc Thesis

Manavendra Nath

Signature of Convener,DPGC

Dedicated to my family

"I have to remind myself that some birds aren't meant to be caged. Their feathers are just too bright. And when they fly away, the part of you that knows it was a sin to lock them up does rejoice."

–***Shawshank Redemption(Movie)***

Acknowledgements

I am incredibly grateful to my supervisor Prof. Subhendu Rakshit for his assistance and guidance throughout my M.Sc. period. Without his support my M.Sc journey could not be completed. His way of observing the problem and breaking it down motivates me to look at problems in different way. I am completing M.Sc with much more maturity in physics as compared to when I came and his role is magnificent in this. I am also thankful to all our teachers for their kind and valuable suggestion.

I am also thankful to Phd scholar Dhruv Ringe for clearing my doubts related to thesis, academics and life. Despite having busy schedules they always took out time to help me.

I would like to thank my family as they are the reason of my existence. Their support is always there for me and it makes me feel blessed. Words can't describe their love for me and my love for them.

At last I want to thank some lovely people I met here and will be in my hearts forever Deepak, Shivansh, Nilesh, Rahul, Praveen and amazing juniors and many others.

List of Figures

Abstract

The Gallium detectors are one of the low energy radiochemical neutrino detectors using ^{71}Ga . They are used to detect the low energy solar (pp) neutrinos. In order to check the overall efficiency of the detectors the calibration experiment were performed using the known neutrino sources. However these calibration experiments results in the anomaly known as "The Gallium Anomaly" which states that the event rates measured are lower than the expected in the neutrino detection experiment by gallium detectors. We will try to tackle the problem by considering the Neutral current channel in neutrino detection experiment by gallium detectors. The motivation for doing this is because of the lower measured event rate than expected. It means there is a problem for missing neutrinos. The idea is there could be the possibility that may be huge flux of neutrinos are scattered by the nucleus via elastic scattering. Here event rate refers to the germanium counting rate. We first try to understand the problem and tried to look for several reasons that could be the reason for the anomaly. We first try to find the cross-section for elastic neutrino nucleon scattering. However in the real problem we have to deal with the whole nucleus but not only with single nucleon. In order to deal with whole nucleus we used the "Coherent Elastic Neutrino Nucleus interaction". We used the coherent elastic channel because the neutrinos produced by source in gallium experiments are of keV range. At these low energy neutrino the coherent elastic scattering dominates.

Contents

CHAPTER 1

Solar Neutrino Problem

1.1 Introduction

The neutrino flux of electron neutrino ν_e emitted by the sun is very high , named solar neutrinos. They contain data regarding the star's internal composition and the energy source located within the core. In 1967, the first experiment to look for solar neutrinos was launched. In over half a century, the community that works with solar neutrinos has made great strides. Seven detectors have looked for solar neutrinos in various energy windows and using various methodologies. The field has gathered basic data on astrophysics and neutrino physics. The sun neutrino problem (SNP) was raised by early neutrino observations. There were fewer solar neutrinos found than anticipated. Initially, it was unclear if novel neutrino physics or an unidentified effect in astrophysics may be the source of the missing solar neutrinos. About thirty years passed before the nature of this problem. Within the paradigm of mixing of neutrino and interaction of neutrino in matter, the collected data offered a solution.

The gallium detector was one of several devices that could detect low-energy neutrinos. Finding the flow for neutrinos with low energy generated in the major proton-proton (pp) reaction became crucial because of the suppression of the flux of high energy neutrinos from the sun. The neutrino capture reaction is the foundation of these investigations. $^{71}Ga(\nu_e, e^-)^{71}Ge$ possesses a very low 233 keV threshold. They consequently offer the sole practical way to detect low-energy neutrinos at this time are sensitive to the pp neutrinos with low energy, whose energy is 423 keV[1]. SAGE findings are $66.9^{7.1+5.4}_{-6.8-5.7}$.The Bahcall-Pinsonneault solar model predicts 129^{+8}_{-6} SNU for Ga metal and 77.5 ± 6.2 for $GaCl_3$. The gallium experiment depends on the ability to collect, purify, and count a few radioactive element atoms created by interactions of neutrinos inside of several tons of target material with well-established efficiency[2]. .At the start of each exposure, 700 mg of a stable Ge carrier is introduced to Ga in order to gauge the extraction efficiency; nevertheless, even with this addition, the separation factor between Ge and Ga remains at 1 atom in 10^{11}[2]. This remarkably strict criterion begs the question of how generally understood the numerous efficiencies that are integrated into the end product are. Since the beginning, it has been known that if the detector is exposed to a known flux of neutrinos with low energy, a thorough examination of its whole operation—that is, its chemical extraction efficiency, counting efficiency, and analysis technique—will be conducted[3]. Such a test not only confirms the detector's functionality but also removes any serious doubts about the possibility that gallium's so-called "hot atom chemistry" could chemically bind ^{71}Ge atoms produced by inverse beta decay in a way that produces an extraction efficiency that differs from the natural Ge carrier. Stated differently, the experiment examines a basic tenet of radiochemical research, namely, the equality of the extraction efficiency between atoms generated through neutrino interactions and carrier atoms. These experiments found a ^{71}Ge rate of production of 0.87 ± 0.05 of that expected, employing ^{51}Cr and ^{37}Ar positioned near the center of their Ga targets.

Via reaction $^{71}Ga(\nu_e, e^-)^{71}Ge$, neutrinos from the Sun were detected by the radiochemical experiments SAGE and GALLEX. Numerous outside interested parties as well as collaborations conducted in-depth investigations on the cross-section, extraction efficiency, and counting efficiencies as a result. This difference between measured and projected rates is what is called the "gallium anomaly." The interpretation of this anomaly is the $\nu_e \rightarrow \nu_s$ oscillation. Despite the limited statistical evidence of a divergence from expectation, approximately $2\sigma - 3\sigma$, the evidence has remained, indicating the need for additional research. Additionally, this is a useful method to look for sterile neutrinos (ν_s) . The (BEST) was intended to be an oscillation experiment that took place over two distances. The average value of the capture rate of neutrino in relation to the predicted value for all Ga experiments is 0.80 ± 0.05. Following the BEST observations, the Ga anomaly appears more pronounced.

In section(2) we will discuss the solar neutrino problem provided by different experiments in solar neutrino. In particular, we will focus on the Gallium detector experiments. In section(3) we will describe the collaboration experiments GALLEX and SAGE which used artificial sources of neutrinos and discuss the results obtained by these detectors which gave rise to gallium anomaly. In section(4) we will define the gallium anomaly. In section(5) we will discuss the

BEST experiment after which the statistical significance of the anomaly was enhanced. In section(6) we will discuss the ways found in the literature to resolve the anomaly. In section(7) we will summarize the report and finally in section(8) we will discuss the future goals.

1.2 Solar Neutrino problem

The difference between the observed and expected solar neutrino fluxes from the mainstream solar model is known as the solar neutrino problem. Seven detectors have looked for solar neutrinos in various energy windows and using various methodologies.

1.2.1 Solar neutrinos

The sun produces neutrino from the so-called proton-proton(pp) chain reaction. The chain reaction goes as follows,

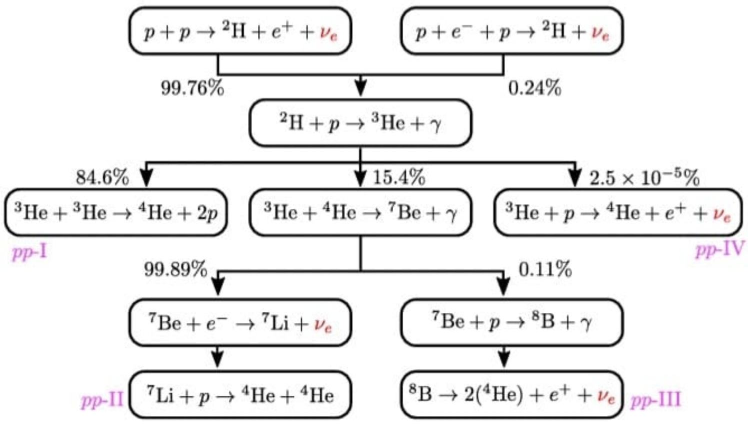

Figure 1.1: pp chain reaction

The solar standard model predicted the solar neutrino flux for neutrinos produced via different reactions. The spectrum of neutrino produced from the sun as predicted by the SSM is given as follows,

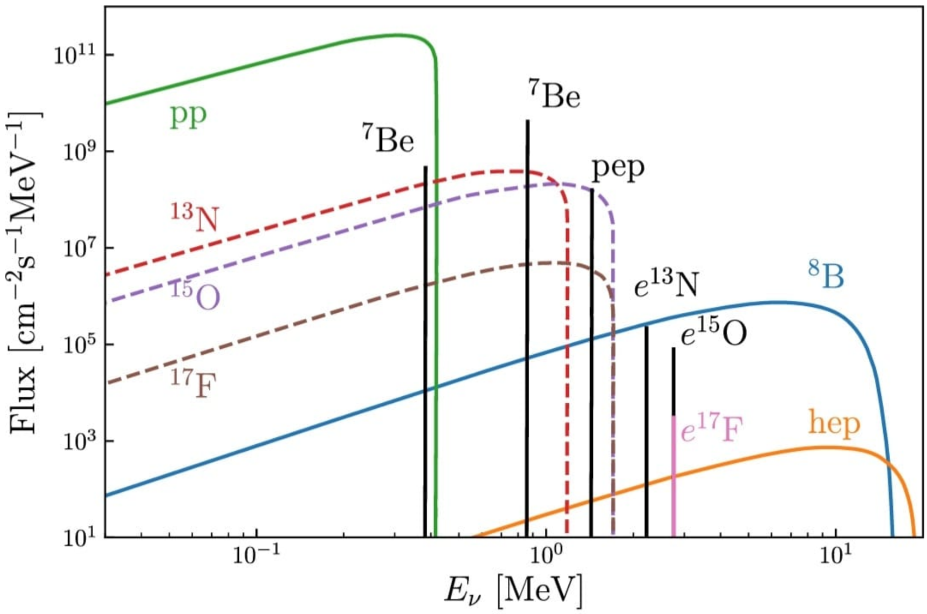

Figure 1.2: Solar neutrino energy spectrum

The energy of neutrino produced by the different reactions is given in the table below,

Reaction	Energy(MeV)
pp	<0.423
pep	1.442
hep	<18.77
^{7}Be	0.862(89%) + 0.38(11%)
^{8}B	<15.5
^{13}N	<1.199
^{15}O	<1.74
^{17}F	<1.732

1.2.2 Detection of solar neutrinos

Different methods have been used to look for solar neutrinos. Over the course of these roughly 50 years, the ability to detect unusual events has significantly increased due to a number of experimental challenges. In reality, during the past few years, the experimental expertise gained from the hunt for solar neutrinos has been applied directly to the search for dark matter, where solar neutrinos will eventually turn into an irreducible background source.

The detectors used for solar neutrino detectors with their characteristics are given in the table below,

Detector	Active mass	Threshold(MeV)	Data taking
Homestake	615 tons, C_2Cl_4	0.184	1967-1994
Kamiokande II/III	3 kton, H_2O	9/7.5/7.0	1986-1995
SAGE	50 tons, molten metal Ga	0.233	1990-2007
GALLEX	30.3 tons, $GaCl_3 - HCl$	0.233	1991-1997
GNO	30.3 tons, $GaCl_3 - HCl$	0.233	1998-2003
Super-Kamiokande	50 ktons H_2O	5/7/4.5/3.5	1996-present
SNO	1 Ktons D_2O	6.75/5/6	1996-2006
BOREXINO	300 tons, C_9H_{12}	0.2	2007-present

The ^{37}Cl experiment

For twenty years, the ^{37}Cl experiment was the sole operational detector for solar neutrinos, collecting data from 1967 to 1994. The following is the fundamental method of detection:

$$\nu_e \ + \ ^{37}_{17}Cl \ \rightarrow \ e^- \ + \ ^{37}_{18}Ar$$

The resulting unstable ^{37}Ar decays back to with a 0.814 MeV is the energy threshold for the equation above. With a half-life time of 30.03 days, the generated ^{37}Ar decays back to ^{37}Cl due to its instability. The purpose of the detection system is to gather the argon atoms and calculate the associated radioactivity.

Kamiokande II/III

In the Japanese Kamioka mine, the Kamiokande detector was constructed in 1983. The experiment's primary objective was to use a 3-kton imaging water Cherenkov detector to look for proton decay. The detector was modified in 1985 to look for solar neutrinos. 1986 marked the end of the improvement. The ^{37}Cl experiment had been collecting data for almost 20 years at this point. Water's radioactivity had to be decreased and the detection threshold had to be adjusted below 10 MeV in order to observe neutrinos from the sun with a water Cherenkov detector. The improved detector, dubbed Kamiokande-II, was operational from 1986 and 1990. The fundamental process for this detector is given by:

$$\nu \ + \ e^- \rightarrow \nu \ + \ e^-$$

The Cherenkov light that is created as electrons recoil is known as the neutrino signal.

The ^{71}Ga experiment

Based on the capture reaction, the ^{71}Ga experiments are radiochemical studies:

$$\nu_e \ + \ ^{71}_{31}Ga \ \rightarrow \ e^- \ + \ ^{71}_{32}Ge$$

The reaction mentioned above has a threshold of 0.233 MeV.The maximum energy of pp solar neutrino is 0.42 MeV. The pp solar neutrino can be detected by the above interaction process. There have been two experiments conducted using ^{71}Ga: SAGE at Baksan Laboratory in Russia and GALLEX at Gran Sasso Laboratory in Italy. This technique was believed to be the exclusive means of detecting pp solar neutrinos at the time the gallium experiments were designed. Given that pp neutrino fluxes are correlated with sun luminosity, measuring these neutrinos would have been an essential test to determine the origin of the SNP. With a typical life of 16.5 days, the ^{71}Ge generated by solar neutrino interactions decays. Using the SSM, the estimated capture rate is 128 ± 5 SNU. From 1991 to 1997, solar neutrinos were measured by GALLEX. GALLEX became the Gallium Neutrino Observatory (GNO) in 1998. GNO operated till the year 2003. The total results of GALLEX and GNO added together, which span a period of 12 years and equate to 123 solar neutrino runs, equal $67.13^{+4.64}_{-4.63}$ SNU. GALLEX + GNO measures a solar neutrino deficit of roughly 50 %.

Superkamiokande

The second-generation solar neutrino detector, Super-Kamiokande (SK), is situated next to Kamiokande in the Kamioka mine at a depth of 2700 meters west of Earth. A 50 Ktons water Cherenkov detector is called SK. The fundamental technique for detection in SK is comparable to Kamiokande-II/III.

$$\nu \ + \ e^- \rightarrow \nu \ + \ e^-$$

The recoiling electrons in the above process produces cherenkov radiation. These radiation works as the detection signal for the detection of neutrinos.

SNO

For simultaneously detecting the solar neutrinos through charged current and neutral-current interactions, the Sudbury Neutrino Observatory (SNO) was constructed. SNO is a heavy water

(D2O)-based Cherenkov detector. Through the following mechanisms, the heavy water makes solar neutrino observation possible:

$$\nu_e \;+\; e^- \;\rightarrow\; \nu_e \;+\; e^-$$

$$\nu_e \;+\; d \;\rightarrow\; e^- \;+\; p \;+\; p$$

$$\nu_e \;+\; d \;\rightarrow\; e^- \;+\; n \;+\; p$$

Elastic Scattering (ES) interaction is the initial process, which functions similarly to previous detectors. The second process, which analyzes any variation influencing the neutrino flux and spectrum created in the Sun's core once detected at 1 A.U. distance and after propagating through the star's interior, is solely sensitive to ν_e through a CC interaction. The target mass's electron interactions produce the visible energy. Through an interaction with neutral current, the third step is sensitive to all neutrino flavors. The target mass's neutron interactions are the indirect source of the visible energy. The threshold for the CC(NC) procedure is 1.442(2.224) MeV.

BOREXINO

The Borexino detects the solar neutrinos of energy below 5 MeV in real time. The contamination in the target water, ^{238}U and ^{232}Th, would make it difficult for Cherenkov experiments to decrease the detection threshold below around 5 MeV; limitations were set at the level of 10^{-14} g(U, Th)/g. It was suggested that levels of 10^{-16} g(U, Th)/g, which are low enough to detect solar neutrinos by elastic scattering process in the MeV range, may be achieved by purifying an organic liquid scintillator. A neutrino interaction via elastic scattering in a liquid scintillator will result in isotropic scintillation light emission with a yield of order 104 photons/MeV, which is significantly higher than in a Cherenkov detector.

1.2.3 Results of different detectors

The flux measured for solar neutrinos by the detectors is given below: [4]

Experiment	DATA	DATA/SSM
Homestake	2.56±0.23 SNU	0.32 ± 0.05
GALLEX/GNO/SAGE	66.2 ± 3.1 SNU	0.52 ± 0.03
SK-I + II + III + IV	$2.345 \pm 0.039 \times 10^6\ cm^{-2}s^{-1}$	0.42 ± 0.06
SNO	$2.04 \pm 0.18 \times 10^6\ cm^{-2}s^{-1}$	0.36 ± 0.06

CHAPTER 2

Calibration experiments: GALLEX and SAGE

2.1 Need of Calibration experiments

Similar to other solar neutrino experiments, the gallium experiment depends on the ability to collect, purify, and count a few radioactive element atoms created by the interactions of neutrino inside of several tons of target material with well-established efficiency[2]. This indicates the removal of a few tens of ^{71}Ge atoms from 53×10^{29} atoms of Ga in the instance of 60 tons of Ga[2]. At the start of exposure, 700 mg of a stable Ge carrier is introduced to Ga in order to gauge the extraction efficiency; nevertheless, even with this addition, the separation factor between Ge and Ga remains at 1 atom in 10^{11}[2]. This remarkably strict criterion begs the question of how generally understood the numerous efficiencies that are integrated into the end product are. Since the beginning, it has been known that if the detector is exposed to a known flux of low-energy neutrinos, a thorough examination of its whole operation[3]. Such a test not only confirms the detector's functionality but also removes any serious doubts about the possibility that gallium's so-called "hot atom chemistry" could chemically bind ^{71}Ge atoms produced by inverse beta decay in a way that produces an extraction efficiency that differs from the natural Ge carrier. Stated differently, the experiment examines a basic tenet of radiochemical research, namely, the equality of the extraction efficiency between atoms generated through neutrino interactions and carrier atoms.

2.2 Source of neutrinos for GALLEX and SAGE

Gallex did two experiments with (^{51}Cr) source and SAGE also did two experiments with (^{51}Cr) and (^{37}Ar) sources. These sources decay via the electron capture process and produce monoenergetic neutrinos. They were placed at the center of the detector.

2.2.1 ^{51}Cr source

The ^{51}Cr source produces monoenergetic neutrinos via the following process of electron capture:

$$^{51}Cr \ + \ e^- \ \rightarrow \ ^{51}V \ + \ \nu_e$$

Neutron capture on ^{50}Cr produces ^{51}Cr, which has a half-life of 27.706±0.007 days. Four monoenergetic lines make up the neutrino spectrum, aside from the low-intensity internal bremsstrahlung.[2] [5].

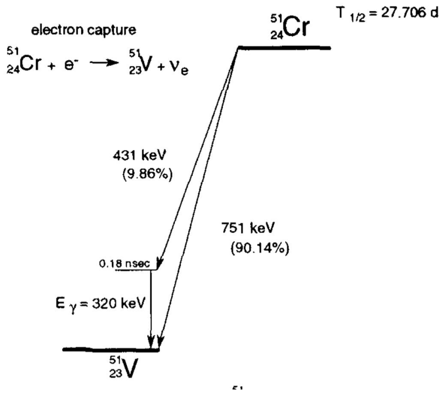

Figure 2.1: Chromium decay via electron capture

2.2.2 ^{37}Ar source

The following figure illustrates how ^{37}Ar decays to ^{37}Cl, with a half-life of 35.04 $\pm$ 0.04 days. The Q value is 813.5 keV, and the decay is exclusively due to electron capture[6].

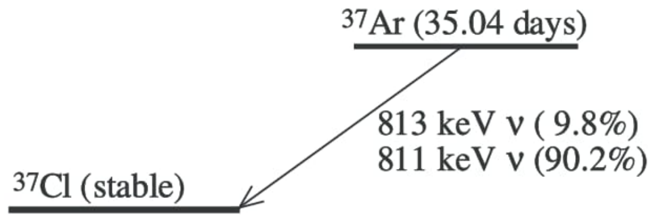

Figure 2.2: Argon decay via electron capture

CHAPTER 3

The Gallium anomaly

3.1 Results from GALLEX and SAGE

It has been observed that the ratio of observed to expected event rates are smaller than unity. The ratios are given in the table below:

Experiment	Result
GALLEX(Cr1)	0.95 ± 0.11 ,
GALLEX(Cr2)	0.81 ± 0.11
SAGE(Cr)	0.95 ± 0.12
SAGE(Ar)	0.790 ± 0.095

As we can see the rate of observed counting rates of Germanium atoms is less than the predicted rates of germanium atoms. The production of less number of germanium atoms for the given activity of germanium indicates that there is a deficiency of neutrinos observed at the detector.

To summarize the gallium anomaly, measurements of the charged-current capture rate of neutrinos on ^{71}Ga from strong radioactive sources have produced findings that are lower than anticipated. These results are based on theory reinforced by known strength of the main transition[7].

3.2 Enhancement of statistical significance of anomaly with BEST experiment

These experiments reported a ^{71}Ge production rate of 0.87 $\pm$ 0.05 of that expected, employing ^{51}Cr and ^{37}Ar positioned at the middle of their Ga targets. Numerous outside interested parties as well as collaborations conducted in-depth investigations on the cross-section, extraction efficiency, and counting efficiencies as a result. The "gallium anomaly" is defined as the difference between the measured and predicted rates, and it has been explained in terms of $\nu_e \rightarrow \nu_s$ oscillations. Even while there is little statistical support for a divergence from expectation—roughly 2σ–3σ—it has remained consistent, indicating the need for additional research.Because there was only one target used in the prior source measurements, it was necessary to compare the recorded rate to the theoretical value. The BEST was intended to be an oscillation experiment that took place over two distances. a With a diameter of 133.5 cm, an inner spherical chamber holds 7.4691 tons of Ga. A cylindrical outer chamber measuring 234.5 cm in height and 218 cm in diameter holds 39.9593 $\pm$ 0.0024 tons of Ga. By positioning the ^{51}Cr source at the center and concurrently irradiating both volumes, it was possible to measure the ^{71}Ge production rate at two different distances. The Ga was fed into reactors for the extraction chemical after exposure. The activity of the source was 3.414$\pm$0.008 MCi [8] [9].

Result

For the measured-to-expected ratios, the two BEST findings are R_{out}. = 0.77 $\pm$ 0.05, and R_{in} = 0.79 $\pm$ 0.05.[10] The average value of the neutrino capture rate in relation to the predicted value for all Ga experiments is 0.80 $\pm$ 0.05. Following the BEST observations, the Ga anomaly seems more pronounced.

CHAPTER 4

Several Attack vectors to the anomaly.

4.1 Introduction

R = N_{meas}/N_{pred} = 0.803 ± 0.035 is the present status of the[3] disparity, which is generally described as the number of measured to expected ratio of occurrences of events. The mixing of active neutrinos and potential sterile states has been proposed as one explanation for the gallium anomaly. Reactor experiments really seemed to confirm this theory for a while by showing a comparable deficiency. But more recently, it has become clear that errors in the measurement of beta spectra from nuclear fission, which are utilized as input to reactor neutrino flux estimates, are most likely to blame for the apparent deficiency in the reactor neutrino flux[11].

Therefore, it is more important than ever to look for Standard Model (SM) solutions Finding answers for the gallium anomaly within the Standard Model is consequently more important than ever. A number of attack vectors will be covered, including the calorimetric measurement of the source intensity, the calibration of the radiochemical germanium extraction efficiency, and the observed ^{71}Ge decay rate that is used as input to compute the $\nu_e+^{71}Ga$ cross-section[11]. Although, on the surface, none of these possible single points of failure can account for the anomaly, our analysis calculates the amount of error that supporting measures would need to have in order to fix it. We investigate what would need to happen in circumstances other than the Standard Model (BSM) to account for the gallium anomaly in the second section.

4.1.1 Detection Cross Section

The detection process and the cross section $\sigma(\nu_e +^{71} Ga)$

$$\nu_e \ + \ ^{71}Ga \ \rightarrow \ e^- \ + \ ^{71}Ge$$

has been questioned[11]. In-depth research on $\sigma(\nu_e +^{71} Ga)$ has been done by Bahcall and Haxton, and Semenov. Transitions to the ground state of ^{71}Ge and transitions to excited states of ^{71}Ge, which are only theoretically calculable with significant uncertainties, make up the two contributions. Most importantly, even if the latter contribution is set to zero, the anomaly still exists.[12] For the purpose of predicting $\sigma(\nu_e +^{71} Ga)$, the measured ^{71}Ge half-life is therefore the major component. The following is a discussion of this measurement's robustness.

Measured ^{71}Ge decay rate

The ^{71}Ge half-life has been measured most precisely and thoroughly since 1985[13]. Two distinct experimental approaches were used to conduct six different measurements, all of which produced consistent results. The ^{71}Ge half-life's accepted value is

$$T_{1/2} \ = \ 11.43 \pm \ 0.03 \ \ days$$

This number would still need to increase by around one day (33σ) in order to reduce its importance to below 3 σ , and it would need to be greater by at least two days (67σ) in order to fully explain the gallium anomaly.

Ge-71 decays to new excited of Ga-71

The ground state of the daughter nucleus, ^{71}Ga, is thought to be reached by electron capture in ^{71}Ge. In actuality, the energy of the lowest-lying known excited state of ^{71}Ga is 389.94 ± 0.03 keV, above the ^{71}Ge decay's Q-value of 232.49 ± 0.22 keV. Here, we propose that ^{71}Ga may have another low-lying excited state that has not yet been found. The nuclear matrix element for ground state-to-ground state transitions (which enters the computation of $\sigma(\nu_e +^{71} Ga)$) would have been overstated by the same amount if about 20% fraction of ^{71}Ge entered this state. Taking this prejudice into account could fix the gallium anomaly. Of However, because the state at 390 keV has been detected in a number of nuclear events, including ^{71}Ge decay, it is difficult to understand how the existence of such an excited state could have gone unnoticed.

4.1.2 Source: ^{51}Cr Branching ratios

The estimate of the neutrino flux released by the source is a second essential component of the research at the gallium anomaly's source. To date, the majority of experiments have used a ^{51}Cr source, which is created by irradiating chromium metal that has been enriched in ^{50}Cr with neutrons. By means of electron capture, ^{51}Cr decays.

$$^{51}Cr \ + \ e^{-} \ \rightarrow \ ^{51}V \ + \ \nu_e$$

Having a 27.704 ± 0.004 day half-life. An ^{37}Ar source (electron capture decay to ^{37}Cl, $T_{1/2}$ = 35.011 ± 0.019 days) has only been used by SAGE. But as this measurement only contributes slightly to the total evidence for a neutrino deficit, we will concentrate on $^{51}Cr.$ sources in this article.

The first primary heat sources in these experiments are X-rays which are produced from the de-excitation of the electron shell and the second primary heat source are the gamma rays which are produced from the de-excitation of the daughter nucleus, with the second contribution being significantly greater. The source intensity is measured calorimetrically, and since the decay occurs via electron capture. Rather than populating the ground state, the initial excited state of ^{51}V at 320.0835 ± 0.0004 keV is occupied by ≈ 10% of all ^{51}Cr decays. Furthermore, we observe that the measurement of the source intensity is dependent on only ≈ 10% of all decays, as nearly all heat production is derived from the ≈ 320 keV de-excitation gamma rays. Put otherwise, the source intensity would have been overstated by ≈ 20%, which would have been sufficient to explain the gallium anomaly, if the real branching ratio for decays to the excited state, $BR_{exc} \ = \ BR(^{51}Cr \rightarrow \ \ ^{51}V^{*})$, had merely been bigger by ≈ 2%.

4.1.3 Electron to sterile neutrino transition

The ≈ 20 % deficit of event rates could be due to electron to sterile neutrino transition. This hypothesis was tested by BEST by performing two distance oscillation programs as we already discussed before. Here we will try to find the oscillation parameters $\Delta m^2 - sin^2\theta$ assuming $\nu_e \ \rightarrow \nu_s$ is the origin of the anomaly. The inputs to the $\nu_e \ \rightarrow \nu_s$ formula is provided from the BEST experiment.

Activity of source

The source's active core was composed of 26 irradiated Cr disks that were inserted into a stainless-steel cylinder measuring 4.3 cm in radius and 10.8 cm in height. The cylinder was protected from radiation by a tungsten alloy with a thickness of around 30 mm. The State Scientific Center Research Institute of Atomic Reactors at Dimitrovgrad, Russia, used a reactor to irradiate 4 kg of ^{50}Cr-enriched metal for 100 days in order to create the source. Our selected reference time for the source strength is 14:02 on July 5, 2019, the day the source was brought to the Baksan Neutrino Observatory (BNO) and installed into the two-zone target. At the reference time, the activity (A) is (3.414 ± 0.008) MCi.

Neutrino energy spectrum from ^{51} Cr source

The energies of neutrino produced from ^{51}Cr via electron capture with their branching ratios are summarized in the table below:

Energy(keV)	Branching ratio
747	81.63 %
427	8.95 %
752	8.49 %
432	0.93 %

Cross section $\sigma(\nu_e\ +\ ^{71}Ga)$

The cross-section $\sigma(\nu_e\ +\ ^{71}Ga)$ four different energies neutrinos produces is provided in the table below:

Energy(keV)	Cross section($\times\ 10^{-46}\ cm^2$)
747	60.8
427	26.7
752	61.5
432	27.1

Event rate and oscillation parameter

For a given ν energy (E_ν), the survival probability for two-component oscillation at a distance d is

$$P_{ee} = 1 - \sin^2 2\theta \sin^2 \left(\frac{1.27\Delta m^2[eV^2]d[m]}{E_\nu[MeV]} \right)$$

where θ is the angle defining the mixing between the two neutrino species and Δm^2 is the difference between their squared masses. One way to write the capture rate (r) is

$$r = \int_V F \sum_{i=1}^{4} f_i P_i^{ee} \sigma n d\vec{x}$$

where n is the ^{71}Ga number density $[2.1001 \pm 0.0008 \times 10^{22}\ cm^{-3}]$, F is the flux of ν_e, P_i^{ee} is the oscillation survival probability for the ith neutrino branch with branching fraction f_i, σ is the cross section. This can be expressed as follows: with A representing the source activity and d denoting the separation between the ν_e's emission and absorption,

$$r = \frac{n\sigma A}{4\pi} \int_V \frac{\sum_i [f_i\ P_i^{ee}(d)]}{d^2} d\vec{x}$$

the permitted $\Delta m^2 - sin^2 2\theta$ parameter space, assuming that the gallium anomaly originates from $\nu_e \rightarrow \nu_s$ oscillations. For BEST-only data, $\Delta m^2 = 3.3\ eV^2$ and $sin^2 2\theta = 0.42$ provide the best fit. The conclusion is $\Delta m^2 = 1.25\ eV^2$ and $sin^2 2\theta = 0.34$, including all of the Ga data. The bounds on $sin^2 2\theta_{14}$ derived from the examination of data from solar neutrino experiments and reactor rate data conflict with this result.

CHAPTER 5

Neutrino nucleon neutral current channel:Standard Model.

5.1 The Idea

As we can see that the measured event rate is less than the predicted event rate. If we believe that there is no problem with the experiment then the source of anomaly could be the theoretical calculation made in predicting the event rates. Since the predicted event rate is more than the measured event rate therefore we can assume that may be we have overestimated the cross section of gallium detection reaction.

The neutrino detection process by gallium is based on Charged current interaction. The event rate rates were predicted without taking into account the neutral current channel i.e the elastic scattering channel of neutrino and gallium nucleus. The idea is if the comparable amount of flux of neutrino is passed through the neutral current channel i.e elastic scattering then the flux available for the charged current process will not be the same as flux of neutrino coming from the neutrino source which was taken into account while predicting the event rates by different experiments.

The availability of flux for charged current channel depends upon the cross section of neutral current channel[14]. We will try to calculate the neutral current cross section for neutrino and single nucleon and will see whether the cross is comparable to the charged current cross section.

5.2 Neutral Current Elastic Scattering on Free Nucleons

The neutrino neutral current elastic scattering cross-section on unbound nucleons is first described. This is expressed by the following formula:

$$\nu(q_1, \sigma_1) + N(p_1, \kappa_1) \to \nu(q_2, \sigma_2) + N(p_2, \kappa_2)$$

The differential cross-section in the laboratory frame, ignoring the neutrino mass, can be written as follows:

$$\frac{d\sigma}{dQ^2} = \frac{\langle |M|^2 \rangle}{64\pi m_N^2 E_\nu^2} \tag{5.1}$$

where $Q^2 = -q^2$ is the four-momentum carried by Z^0 , $q = p_2 - p_1 = q_1 - q_2$, Since the particle polarizations are typically not observed, $\langle |M|^2 \rangle$ represents the matrix element squared averaged over the starting and final spin particles, and E_ν represents the neutrino energy.

The nucleon is the only particle that could be seen in the detector. If the first nucleon is at rest, then Q^2 can be expressed using the kinematics of the outgoing nucleon by simply

$$Q^2 = 2m_N T_N$$

where the nucleon's outward kinetic energy is denoted by T_N. Conveniently, this is independent of the nucleon's scattering angle, even if certain tests might not be able to measure it. The matrix element squared can be written using the electro-weak theory's Feynman rules.

$$M = -\left(\frac{ig}{4\cos\theta_W}\right)^2 \bar{\nu}\left(q_2\right)\gamma^\mu\left(1-\gamma_5\right)\nu\left(q_1\right) i\frac{\left(g_{\mu\nu} - q_\mu q_\nu / M_Z^2\right)}{q^2 - M_Z^2} \left\langle N\left(p_2\right)\left|J_Z^\nu\right| N\left(p_1\right)\right\rangle$$

One can substitute the propagator for low momentum transfer ($q^2 < M_Z^2$).

$$-i\frac{\left(g_{\mu\nu} - q_\mu q_\nu / M_Z^2\right)}{q^2 - M_Z^2} \quad \to \quad -i\frac{g_{\mu\nu}}{M_Z^2}$$

Additionally, utilizing the Fermi constant's formulation,

$$G_F = \frac{\sqrt{2}g^2}{8M_W^2} = \frac{\sqrt{2}g^2}{8M_Z^2\cos^2\theta_W}$$

The matrix element's expression can be obtained.

$$M = \frac{i}{2\sqrt{2}} G_F \underbrace{\bar{\nu}\left(q_2\right)\gamma_\mu\left(1-\gamma_5\right)\nu\left(q_1\right)}_{\text{leptonic current}} \underbrace{\left\langle N\left(p_2\right)\left|J_Z^\mu\right| N\left(p_1\right)\right\rangle}_{\text{hadronic current}}$$

The leptonic current has a straightforward expression: it consists of the vector and axial components of the so-called V-A structure. However, because of the strong interactions occurring within the nucleon, the hadronic current is a complicated entity. The hadronic weak neutral current's most prevalent form is

$$\langle N(p_2)|J_Z^\mu|N(p_1)\rangle = \langle N(p_2)|\gamma^\mu \underbrace{F_1^Z\left(Q^2\right) + F_2^Z\left(Q^2\right)\frac{i\sigma^{\mu\nu}q_\nu}{2M_N}}_{Vector\,current} + \underbrace{F_A^Z\left(Q^2\right)\eta^\mu\gamma_5}_{Axial\,current}|N(p_1)\rangle,$$

where $F_1^Z(Q^2)$, $F_2^Z(Q^2)$ and $F_A^Z(Q^2)$ are Dirac, Pauli, and axial vector nucleon weak neutral current form factors, respectively.

The elastic differential cross-section for neutrino-nucleon neutral current can be expressed as[15]

$$\frac{d\sigma}{dQ^2} = \frac{G_F^2 Q^2}{2\pi E_\nu^2}\left(A\left(Q^2\right) + WB\left(Q^2\right) + W^2C\left(Q^2\right)\right) \tag{5.2}$$

where, $W = \frac{4E_\nu}{M_N} - \frac{Q^2}{M_N^2}$

$A(Q^2)$, $B(Q^2)$ and $C(Q^2)$ are the form factors given by,

$$A\left(Q^2\right) = \frac{1}{4}\left[\left(F_A^Z\right)^2(1+\tau) - \left(\left(F_1^Z\right)^2 - \tau\left(F_2^Z\right)^2\right)(1-\tau) + 4\tau F_1^Z F_2^Z\right] \tag{5.3}$$

$$B\left(Q^2\right) = -\frac{1}{4}F_A^2\left(F_1^2 + F_2^2\right), \tag{5.4}$$

$$C\left(Q^2\right) = \frac{M_N^2}{16Q^2}\left[\left(F_A^Z\right)^2 + \left(F_1^Z\right)^2 + \tau\left(F_2^2\right)^2\right]. \tag{5.5}$$

where $\tau = \frac{Q^2}{4M_N^2}$.

The weak neutral current's general manifestation via the weak charged current and electromagnetic current is as follows:

$$J^Z = \frac{1}{2}\tau_3 J - 2\sin^2\theta_W J^{EM}, \tag{5.6}$$

where $\tau_3 = \mathrm{diag}(1,-1)$ and $\sin^2\theta_W = 0.2325$ represent the Weinberg angle. By applying Equation (6) and expanding the charge current to include the isoscalar component (denoted by the index s), the formulas for the nucleon weak neutral current form factors can be expressed as follows:

$$F_i^Z = \left(F_i - F_i^s\right)\frac{\tau_3}{2} - 2\sin^2\theta_W F_i^{EM}, \quad i = 1, 2. \tag{5.7}$$

$$F_A^Z = (F_A - F_A^s)\,\frac{\tau_3}{2} \tag{5.8}$$

The hadronic weak current's vector component is comparable to the electromagnetic current's:

$$\langle N\,|J^{\mu}_{EM}|\,N\rangle = \left\langle N \left|\gamma^{\mu} F_1^{EM} + \frac{i\sigma^{\mu\omega} q_v}{2M_N} F_2^{EM}\right| N\right\rangle.$$

which explains how hadrons and photons couple. The electromagnetic current is retained, of course. In analogy to the electromagnetic vector current, it is therefore assumed that the weak vector current is conserved. The conserved vector current (CVC) hypothesis is the name given to this theory. This results in the following relationship between the vector form factors of the weakly charged current and those of the electromagnetic current for protons and neutrons:

$$F_i = F_i^{EM,p} - F_i^{EM,n}, \quad i = 1, 2. \tag{5.9}$$

Now, F_1^Z and F_2^Z can be expressed using the electromagnetic form factors for protons and neutrons by inserting Eq.(9) into (7) and (8):

$$F_i^Z = \left(\frac{1}{2} - \sin^2\theta_w\right)\left[F_i^{EM,p} - F_i^{EM,n}\right]\tau_s - \sin^2\theta_w\left[F_i^{EM,p} + F_i^{EM,n}\right] - \frac{1}{2}F_i^s, i = 1, 2. \tag{5.10}$$

$$F_A^Z = \frac{\tau_3}{2}F_A - \frac{1}{2}F_A^s. \tag{5.11}$$

Thus, charged lepton scattering can be used to quantify F_1^Z and F_2^Z under CVC. The so-called Sachs form factors are the two significant combinations of the Dirac and Pauli electromagnetic form factors: [16]

$$G_E = F_1^{EM} - \tau F_2^{EM}, \tag{5.12}$$

$$G_M = F_1^{EM} + F_2^{EM}, \tag{5.13}$$

which represent the electric and magnetic form factors of the nucleon. In scattering theory, the current-density distribution is given by the three-dimensional Fourier transform of $G_M\,(Q^2)$, whereas the electric-charge-density distribution within the nucleon is provided by $G_E\,(Q^2)$. Naturally, the electric charges of the protons and neutrons are represented by the variables $G_E^p(0)$ and $G_E^n(0)$, respectively; the anomalous magnetic moments for the protons and neutrons are denoted by the variables $G_M^p(0)$ and $G_M^n(0)$. Consequently,

$$G_E^p(0) = 1 \tag{5.14}$$

$$G_E^n(0) = 0 \tag{5.15}$$

$$G_M^{\mathrm{p}}(0) = 2.793 \tag{5.16}$$

$$G_M^{\mathrm{n}}(0) = -1.91 \tag{5.17}$$

Regarding the Q^2 dependence, the experimental findings are in general in agreement with a dipole form for these form factors:

$$\frac{G_E\left(Q^2\right)}{G_E(0)} = \frac{G_M\left(Q^2\right)}{G_M(0)} = \frac{1}{\left(1 + \frac{Q^2}{M_V^2}\right)^2} \tag{5.18}$$

Hence, the vector mass for both the electric and magnetic form factors is $M_V = 0.843\text{GeV}$. The Dirac and Pauli electromagnetic form factor expressions can be obtained from Equations (12), (13) and (18).

$$F_1^{EM}\left(Q^2\right) = \frac{G_E(0) + \frac{Q^2}{4M^2} G_M(0)}{\left(1 + \frac{Q^2}{4M^2}\right)\left(1 + \frac{Q^2}{M_V^2}\right)^2} \tag{5.19}$$

$$F_2^{EM}\left(Q^2\right) = \frac{G_M(0) - G_E(0)}{\left(1 + \frac{Q^2}{4M^2}\right)\left(1 + \frac{Q^2}{M_V^2}\right)^2} \tag{5.20}$$

A weak charged current can be used to measure the axial isovector form factor. Furthermore, it is thought to hive: a dipole shape

$$F_A = \frac{F_A(0)}{\left(1 + \frac{Q^2}{M_A^2}\right)^2} \tag{5.21}$$

$F_A(0) = g_A = 1.2671$ is measured precisely from neutron beta decay.

$$F_1^s\left(Q^2\right) = \frac{F_1^s(0)}{(1+\tau)\left(1 + \frac{Q^2}{M_V^2}\right)^2}$$

$$F_2^s\left(Q^2\right) = \frac{F_2^s(0)}{(1+\tau)\left(1 + \frac{Q^2}{M_V^2}\right)^2}$$

$$F_A^s\left(Q^2\right) = \frac{F_A^s(0)}{\left(1 + \frac{Q^2}{M_A^2}\right)^2}$$

where $F_1^s(0) = -\frac{1}{5}\langle r_s^2\rangle$, $F_2^s(0) = \mu_s$ and $F_A^s(0) = \Delta$s. Note that $\langle r_s^2\rangle$ is the strange radius, μ_s is the strange magnetic moment of the nucleon, and Δs is the strange quark contribution to the nucleon spin. [17] Experiments using electron scattering with parity violations can provide F_1^s and F_2^s. Recent findings from the HAPPEX-II experiment demonstrate that these odd form factors, which are magnetic and electric, are consistent with 0. Lastly, the neutrino-nucleon neutral current elastic scattering allows the extraction of Δs.

The expression for the NCE cross-sections of protons and neutrons at low Q^2 may now be found:

$$\frac{d\sigma_{vp}}{dQ^2} \sim \quad g_A^2 - 2g_A\Delta s + (\Delta s)^2$$
$$\frac{d\sigma_{vm}}{dQ^2} \sim 1 + g_A^2 + 2g_A\Delta s + (\Delta s)^2.$$

5.3 Result

The maximum value of cross sections calculated from the above formula is given by,

Z	Δs	$\sigma\,(cm^2)$
p	0	7.45×10^{-40}
p	-0.5	1.44×10^{-39}
n	0	1.21×10^{-39}
n	-0.5	1.91×10^{-39}

Table 5.1: Nucleon cross section for $Q = E_\nu$

The cross section for gallium detection reaction is measured as,

$$\sigma_m = 5.39 \times 10^{-45}\,cm^2$$

CHAPTER 6

Coherent Elastic Neutrino Nucleus Scattering

6.1 Introduction

Neutrino scattering using Z^0-boson exchange from bound particles is a powerful tool for testing quantum physics principles and discovering new phenomena. Under some conditions, the contact probability increases as compared to scattering off free particles. Quantum physics concepts explain why this extra factor is proportional to the number of scatterers.The probability of an event is calculated by squaring the absolute value of the sum of amplitudes for indistinguishable routes leading to that outcome. More than four decades ago, Freedman observed neutrino-nucleus scattering, which preserves the nucleus' integrity.

Such interactions result in two unique results.

(i) The nucleus maintains the same quantum state,

(ii) The state has altered. In elastic scatterings, energy transfer to the recoil nucleus is negligible, while in inelastic scatterings, it appears to be nonzero.

The condition of coherent elastic scattering is stated as,

$$|\vec{q}|R_A << 1 \tag{6.1}$$

where R_A is the radius of the nucleus. The form factors vanish at $|\vec{q}| \to \infty$

Neutrinos with energies below tens of MeV preserve nucleon integrity in neutrino-quark interactions with Z^0-boson exchange.

Freedman proposed the phrase "coherent neutrino nucleus scattering" to underline the quadratic dependency of the cross section on the number of nucleons. Neutrino scattering off nucleons was found to have almost equal amplitude phases, explaining the observed relationship.

6.2 What is Coherent scattering?

Coherent waves share the same frequencies, waveforms, and relative phase. Coherence can lead to both constructive and destructive interference. Neutrinos interact with nucleons by scattering. Each scattering off a kth nucleon has an amplitude of A^k.

Assuming definite nucleon coordinates $\vec{x}_k$, translation invariance adds an additional component $e^{i\mathbf{q}\cdot\mathbf{x}_k}$ to A^k, resulting in the total amplitude.

$$A = \sum_{k=1}^{A} A^k \, e^{i\mathbf{q}\cdot\mathbf{x}_k} \tag{6.2}$$

Coherent individual amplitudes occur when the phases $\mathbf{q}\cdot\mathbf{x}_k$ are roughly identical for any k. This is achieved when the condition in Eq. (6.1) is met.

Is it still fair to evaluate coherency when the nucleon's definite location is no longer assumed? Nucleon locations are defined by a multiparticle scalar wave function: $\psi_{n/m}(\mathbf{x}_A..\mathbf{x}_A)$, where the n/m subscripts represent the nucleus's beginning and final states. The amplitude in Equation (6.2) can be generalized as:

$$A_{nn} = \sum_{k=1}^{A} A^k_{nn} \, f^k_{nn}(\mathbf{q}) \tag{6.3}$$

where

$$f^k_{mn}(\mathbf{q}) = < m|e^{i\mathbf{q}\hat{\mathbf{X}}_k}|n > \tag{6.4}$$

$$f^k_{mn}(\mathbf{q}) = \int \left(\prod_{i=1}^{A} d\vec{x}_i \right) \psi^*_m(\mathbf{x}_1 ... \mathbf{x}_A)\psi_n(\mathbf{x}_1 ... \mathbf{x}_A)e^{i\mathbf{q}\cdot\mathbf{x}_k} \tag{6.5}$$

In particular,

$$f^k_{nn}(\mathbf{q}) = \int \left(\prod_{i=1}^{A} d\vec{x}_i \right) |\psi_n(\mathbf{x}_1 ... \mathbf{x}_A)|^2 e^{i\mathbf{q}\cdot\mathbf{x}_k} \tag{6.6}$$

The equation above determines the form factor of a nucleon in the nucleus. The characteristics of the form factor are as follows:

I) $f^k_{nn}(\mathbf{q})$ is independent of the kth nucleon's coordinates. Equation (6.5) integrates out all position variables.

II) $f^k_{nn}(\mathbf{q})$ is unaffected by the index k, despite potential differences in form factors between protons and neutrons. To verify this thesis for fermions and bosons, simply alter the integration variables and account for the wave function's symmetry features when the inputs are interchanged.

Equation (6.6) and the characteristics of $f^k_{nn}(\mathbf{q})$ show that the phases of separate amplitudes in Eq. (6.2) are identical and coherent for any $\mathbf{q}$. This does not imply that the total amplitude is not vanishing at big q, as the form factor $f^k_{nn}(\mathbf{q})$ vanishes. What determines the dependence of $f^k_{nn}(\mathbf{q})$? The fast oscillation of the $e^{i\mathbf{q}\cdot\mathbf{x}_k}$ factor in Eq. (6.5) causes the integrand function to wash out. The physical reason is an incoherent accumulation of waves from a single nucleon's wave function that spans the nucleus' size.

We will now calculate the amplitude square using Eq. (6.2). The amplitude square in terms of diagonal and non-diagonal terms can be expressed as:

$$|A_{nn}|^2 = |f_{nn}(\mathbf{q})|^2 \sum_{k,j} A^k_{nn} A^{j*}_{nn} \tag{6.7}$$

$$|A_{nn}|^2 = |f_{nn}(\mathbf{q})|^2 \left(\sum_k |A^k_{nn}|^2 + \sum_{k \neq j} A^k_{nn} A^{j*}_{nn} \right) \tag{6.8}$$

Diagonal and nondiagonal terms make equal contributions to $|A_{nn}|^2$ and have the same reliance on $\mathbf{q}$. What, then, defines incoherent interactions? These operations involve changing the quantum state of the nucleus ($n \neq m$). Here's a summary of the key parts of a derivation that supports this statement

Assume that the nucleus is originally in the nth quantum state. If the experiment cannot determine the nucleus's ultimate state, the observable should be proportional to the sum of all conceivable final states.

$$|A|^2 = \sum_m |A_{mn}|^2 = |A_0|^2 \sum_{k,j} \sum_m f^k_{mn} f^{j*}_{mn} \tag{6.9}$$

From Eq. (6.5) we can write Eq. (6.9) as:

$$|A|^2 = |A_0|^2 \sum_{k,j} < n|e^{i\mathbf{q}\hat{\mathbf{X}}_j} \sum_m |m >< m|e^{i\mathbf{q}\hat{\mathbf{X}}_k}|n > \tag{6.10}$$

$$|A|^2 = |A_0|^2 \sum_{k,j} < n|e^{i\mathbf{q}\hat{\mathbf{X}}_j}\, e^{i\mathbf{q}\hat{\mathbf{X}}_k}|n > \tag{6.11}$$

We employed the unity operator built of nuclear states. $\sum_m |m><m| = I$

A two-particle correlation function can be defined in terms of real values.

$$G_{nn}(\mathbf{q}) = G(\mathbf{q}) = < n|e^{i\mathbf{q}\hat{\mathbf{X}}_j}\, e^{i\mathbf{q}\hat{\mathbf{X}}_k}|n > \tag{6.12}$$

For k equals j, $G(\mathbf{q}) = 1$. For $k \neq j$.The symmetric features of the nuclear wave function demonstrate that $G(\mathbf{q})$ is independent of k and j. Now using Eq(6.5), (6.8) and (6.11), we get,

$$|A|^2 = |A_0|^2(A + G(\mathbf{q})A(A - 1)) \tag{6.13}$$

$$|A|^2 = |A_0|^2\,(A^2G(\mathbf{q}) + A(1 - G(\mathbf{q}))) \tag{6.14}$$

where A is the number of nucleons. As we can see, $|A|^2$ is quadratically and linearly dependent on A.

6.3 Neutrino Interactions

6.4 Electroweak Lagrangian

The electroweak Lagrangian in the standard model is given by:

$$L_{EW} = -e\sum_i Q_i\bar{\psi}_i\gamma^\mu\psi_i A_\mu - \frac{g}{2\sqrt{2}}\sum_i \bar{\Psi}_i\gamma^\mu(1-\gamma^5)(T_+W_\mu^+ + T_-W_\mu^-)\Psi_i - \frac{g}{2}\cos\theta_W\sum_i \bar{\psi}_i\gamma^\mu(g_i^V - g_i^A)\psi_i Z_\mu \tag{6.15}$$

In equation (6.15), electromagnetic interactions are represented by the photon field A_μ. Photon fields have no mass. Q_i represents the charge of fermions. The second line indicates weak interactions. Weak boson fields (charged) are designated as W_μ^+ and W_μ^-, with mass M_W. $T^\pm$ represents the rising and lowering operators of weak isospin. . The third line depicts weak interactions with the field boson Z_μ, resulting in mass $M_Z = \frac{M_W}{cos\theta_W}$.

In standard model, the neutral current is given by:

$$J_\mu^{NC} = \sum_i 2\left(g_i^L\bar{\psi}_{L_i}\gamma^\mu\psi_{L_i}\right) + \sum_i 2\left(g_i^R\bar{\psi}_{R_i}\gamma^\mu\psi_{R_i}\right) \tag{6.16}$$

$$J_\mu^{NC} = \sum_i \bar{\psi}_i\gamma^\mu(g_i^V - g_i^A)\psi_i \tag{6.17}$$

The chiral projections are:

$$\psi_{Li} = P_L\psi_i = \frac{1-\gamma^5}{2}\psi_i \tag{6.18}$$

$$\psi_{Ri} = P_R\psi_i = \frac{1+\gamma^5}{2}\psi_i \tag{6.19}$$

and

$$g_V^i = g_L^i + g_R^i \tag{6.20}$$

$$g_A^i = g_L^i - g_R^i \tag{6.21}$$

Here, $g_{L,R}^i$ are determined by the quantum numbers of the corresponding fermions under SU(2)L × U(1)Y:

$$g_L^\nu = \frac{1}{2}, \quad g_R^\nu = 0, \quad g_L^e = -\frac{1}{2} + sin^2\theta_W, \quad g_R^e = sin^2\theta_W \tag{6.22}$$

$$g_L^u = \frac{1}{2} - \frac{2}{3}sin^2\theta_W, \quad g_R^u = -\frac{2}{3}sin^2\theta_W, \quad g_L^d = -\frac{1}{2} + \frac{1}{3}sin^2\theta_W, \quad g_R^d = \frac{1}{3}sin^2\theta_W \tag{6.23}$$

At low energies, the effective NC interaction is

$$L_{NC} = \frac{G_F}{\sqrt{2}} J_\mu^{NC} J_{NC}^\mu \tag{6.24}$$

6.5 Evaluating the Amplitude square ($|M|^2$)

6.5.1 The Amplitude M.

The Feynman diagram for neutrino nucleus scattering is shown below.

Assumptions for Nucleus:

- The nucleus must be in a ground state.
- The nucleus must be spherically symmetric so that interaction does not disrupt parity.

After using the Feynman rules, the amplitude becomes:

$$iM_{ss'} = -i\frac{g}{2cos\theta_W} g_L^\nu \bar{u}_{s'}(p_3)\gamma^\mu(1-\gamma^5)u_s(p_1)\left[-i\frac{g_{\mu\nu} - \frac{p_\mu p_\nu}{M_Z^2}}{q^2 - M_Z^2}\right] J_{nuc}^\nu \tag{6.25}$$

The initial and final states of particles are represented by $u_s(p_1)$ and $\bar{u}_{s'}(p_3)$. J_{nuc}^ν is the nuclear current.

J^{ν}_{nuc} can be written as,

$$J^{nuc}_{\nu} = \lambda(p_2 + p_4)^{\nu} \tag{6.26}$$

λ represents poor coupling strength. To determine the value of λ, the neutral current component of L_{EW} will be evaluated.

Because nuclei only contain quarks, J^{μ}_{NC} will contribute to J^{ν}_{nuc} as a quark part.

Assumptions for parity conservation:

$$\bar{u}^L \gamma^{\mu} u^L = \bar{u}^R \gamma^{\mu} u^R \tag{6.27}$$

$$\bar{d}^L \gamma^{\mu} d^L = \bar{d}^R \gamma^{\mu} d^R \tag{6.28}$$

For the d (down quark) and u (up quark) part of J^{μ}_{NC}:

$$J^{\mu}_{NC} = g^u_V \bar{u} \gamma^{\mu} u + g^d_V \bar{d} \gamma^{\mu} d \tag{6.29}$$

Contributions to weak couplings are $2cos\theta_W \cdot g^u_V$ from up quark and $2cos\theta_W \cdot g^d_V$ from down quark.

A nucleus A(Z,N) has $n^d = 2N + Z$ down quarks and $n^u = 2Z + N$ up quarks. The weak coupling constant λ becomes:

$$\lambda = n^u \frac{g}{2cos\theta_W} g^u_V + n^D \frac{g}{2cos\theta_W} g^d_V \tag{6.30}$$

$$\lambda = \frac{g}{2cos\theta_W} \left[n^u \left(\frac{1}{2} - \frac{4}{3} sin^2\theta_W \right) + n^d \left(\frac{1}{2} + \frac{2}{3} sin^2\theta_W \right) \right] \tag{6.31}$$

$$\lambda = \frac{g}{2cos\theta_W} \frac{1}{2} [(1 - 4sin^2\theta_W) Z - N] \tag{6.32}$$

$$\lambda = \frac{g}{2cos\theta_W} \frac{1}{2} Q_W \tag{6.33}$$

Q_W represents the nucleus's weak charge. The present nucleus is viewed as a point-like particle. To count the inner structure of nuclei, multiply the current by a form factor $F(q^2)$.

$$J^{\nu}_{nuc} = \lambda(p_2 + p_4)^{\nu} F(q^2) \tag{6.34}$$

Inserting this result in (7.11).

$$iM_{ss'} = -\frac{g^2}{8cos^2\theta_W} Q_W g_L^\nu \bar{u}_{s'}(p_3)\gamma^\mu(1-\gamma^5)u_s(p_1)\left[\frac{g_{\mu\nu} - \frac{p_\mu p_\nu}{M_Z^2}}{q^2 - M_Z^2}\right](p_2+p_4)^\nu F(q^2) \tag{6.35}$$

At the low energies, when $q^2 << M_Z^2$, the Z boson propagator becomes:

$$\frac{g_{\mu\nu} - \frac{p_\mu p_\nu}{M_Z^2}}{q^2 - M_Z^2} = -\frac{g_{\mu\nu}}{M_Z^2} \tag{6.36}$$

With that approximation, the interaction can be expressed in the form of equation (6.24).

$$iM_{ss'} = -\frac{g^2}{8\cos^2\theta_W M_Z^2} Q_W g_L^\nu \bar{u}_{s'}(p_3)\gamma^\mu(1-\gamma^5)u_s(p_1)(p_2+p_4)_\mu F(q^2) \tag{6.37}$$

Since $M_W = M_Z cos\theta_W$ and $G_F/\sqrt{2} = g^2/8M_W^2$

$$iM_{ss'} = -\frac{G_F}{\sqrt{2}} Q_W g_L^\nu \bar{u}_{s'}(p_3)\gamma^\mu(1-\gamma^5)u_s(p_1)(p_2+p_4)_\mu F(q^2) \tag{6.38}$$

6.5.2 The Amplitude square $|M|^2$

To get $|M|^2$, M with $M^\dagger$ will be multiplied and summed over final states.

$$|M|^2 = \Sigma_{ss'}(MM^\dagger) = \frac{G_F^2}{2} Q_W^2 (g_L^\nu)^2 (p_2+p_4)_\mu (p_2+p_4)_\nu \bar{u}^{s'}(p_1)\gamma^\mu(1-\gamma^5)u^s(p_3)\bar{u}^s(p_3)\gamma^\nu(1-\gamma^5)u^{s'}(p_1)[F(q^2)]^2 \tag{6.39}$$

Now Casimir's trick and completeness relation will be used.

$$\sum [\bar{u}_1\gamma^\mu v_2]\,[\bar{v}_2\gamma^\nu u_1] \tag{6.40}$$

$$\sum_{\sigma_1\sigma_2} \bar{u}_{1\alpha}\gamma^\mu_{\alpha\beta} v_{2\beta}\bar{v}_{2\gamma}\gamma^\nu_{\gamma\delta} u_{1\delta} \tag{6.41}$$

Now $u_{1\delta}$ can be moved to the front. It is just a number so it commutes with everything.

$$\sum_{\sigma_1\sigma_2} u_{1\delta}\bar{u}_{1\alpha}\gamma^\mu_{\alpha\beta} v_{2\beta}\bar{v}_{2\gamma}\gamma^\nu_{\gamma\delta} \tag{6.42}$$

Using Completeness relation:

$$\sum_{\sigma_1} u_{1\delta}\bar{u}_{1\alpha} = (\not{p}_3 + m_1)_{\delta\alpha} \tag{6.43}$$

$$\sum_{\sigma_1} v_{2\beta}\bar{v}_{2\gamma} = (\not{p}_4 - m_2)_{\beta\gamma} \tag{6.44}$$

Which turns the sum into:

$$(\not{p}_3 + m_1)_{\delta\alpha}\gamma^{\mu}_{\alpha\beta}(\not{p}_4 - m_2)_{\beta\gamma}\gamma^{\nu}_{\gamma\delta} = \mathrm{Tr}\left[(\not{p}_3 + m_1)\gamma^{\mu}(\not{p}_4 - m_2)\gamma^{\nu}\right] \tag{6.45}$$

6.5.3 Trace Calculation for neutrino part

Now we will try to calculate the following term extracted from eqn(6.39):

$$S = \bar{u}^{s'}_{\alpha}(p_1)\gamma^{\mu}_{\alpha\beta}(1-\gamma^5)_{\beta\gamma}u^{s}_{\gamma}(p_3)\bar{u}^{s}_{\delta}(p_3)\gamma^{\nu}_{\delta\sigma}(1-\gamma^5)_{\sigma\rho}u^{s'}(p_1)_{\rho} \tag{6.46}$$

Bringing $u^{s'}(p_1)_{\rho}$ to the forefront and applying the completeness relation: u^s and $u^{s'}$ represent particles.

$$\sum_{s'} u^{s'}_{\rho}(p_1)\bar{u}^{s'}_{\alpha}(p_1) = (\not{p}_1 + m)_{\rho\alpha} \tag{6.47}$$

$$\sum_{s} u^{s}_{\gamma}(p_3)\bar{u}^{s}_{\delta}(p_3) = (\not{p}_3 + m)_{\gamma\delta} \tag{6.48}$$

The above sum turns into:

$$S = (\not{p}_1 + m)_{\rho\alpha}\gamma^{\mu}_{\alpha\beta}(1-\gamma^5)_{\beta\gamma}(\not{p}_3 + m)_{\gamma\delta}\gamma^{\nu}_{\delta\sigma}(1-\gamma^5)_{\sigma\rho} \tag{6.49}$$

$$S = Tr[\not{p}_1\gamma^{\mu}(1-\gamma^5)\ \not{p}_3\gamma^{\nu}(1-\gamma^5)] + \mathrm{Tr}[m^2\gamma^{\mu}(1-\gamma^5)\gamma^{\nu}(1-\gamma^5)] \tag{6.50}$$

Using Feynman calculus we get:

$$S = 8(p_1^{\mu}p_3^{\nu} + p_1^{\nu}p_3^{\mu} - g^{\mu\nu}p_1\cdot p_3 - i\epsilon^{\rho\mu\sigma\nu}p_{1\rho}p_{3\sigma}) \tag{6.51}$$

Substituting the above result back into eqn(6.39), we get

$$|M|^2 = 4G_F^2Q_W^2[F(q^2)]^2(g_L^{\nu})^2[2p_1\cdot(p_2+p_4)p_3\cdot(p_2+p_4)-(p_2+p_4)^2p_1\cdot p_3-i\epsilon^{\rho\mu\sigma\nu}p_{1\mu}(p_1+p_2)_{\nu}p_{3\rho}(p_2+p_4)_{\sigma}] \tag{6.52}$$

$$\begin{aligned}|M|^2 = 4G_F^2Q_W^2[F(q^2)]^2(g_L^{\nu})^2\,&[(p_1\cdot p_2)(p_3\cdot p_2) + (p_1\cdot p_2)(p_3\cdot p_4) + (p_1\cdot p_4)(p_3\cdot p_2)\\ &+(p_1\cdot p_4)(p_3\cdot p_4) - (M^2 + p_2\cdot p_4)(p_1\cdot p_3)\big]\end{aligned} \tag{6.53}$$

6.5.4 Calculation of Kinematics

We will do the kinematics in the lab frame. The kinematic variables are given as follows:

$$p_1 = (E_\nu, \vec{p_1}) \tag{6.54}$$

$$p_2 = (M_A, 0) \tag{6.55}$$

$$p_3 = (E_\nu - T, \vec{p_3}) \tag{6.56}$$

$$p_4 = (T + M_A, \vec{p_4}) \tag{6.57}$$

$$q = p_1 - p_3 = p_2 - p_4 = (T, \vec{q}) \tag{6.58}$$

The four vector product is given by,

$$p_3 \cdot p_4 = \frac{1}{2}\left[(p_3 + p_4)^2 - p_3^2 - p_4^2\right] = \frac{1}{2}\left[(p_1 + p_2)^2 - M_A^2\right] = E_\nu M_A \tag{6.59}$$

$$p_1 \cdot p_2 = E_\nu M_A \tag{6.60}$$

$$p_3 \cdot p_2 = (E_\nu - T)M_A \tag{6.61}$$

$$p_4 \cdot p_2 = (T + M_A)M_A \tag{6.62}$$

$$p_3 \cdot p_1 = (p_4 + p_3 - p_2) \cdot p_3 = TM_A \tag{6.63}$$

$$p_4 \cdot p_1 = p_1 \cdot (p_1 + p_2 - p_3) = M_A(E_\nu - T) \tag{6.64}$$

$$q^2 = (p_1 - p_3)^2 = -2TM_A \tag{6.65}$$

Then the Matrix amplitude square becomes:

$$|M|^2 = 32G_F^2 M_A^2 E_\nu^2 Q_W^2 (g_\nu^L)^2 \left[1 - \frac{T}{E_\nu} - \frac{M_A T}{2E_\nu^2}\right] F^2 \tag{6.66}$$

6.6 Differential and Total cross section

Now we will apply the Fermi's Golden Rule to differential cross-sections in lab frames for momentum transfer.

$$\frac{d\sigma}{dq^2} = -\frac{|M|^2}{64\pi E_\nu^2 M_A^2} \tag{6.67}$$

The differential cross-section for coherent neutrino-nucleus scattering is as follows:

$$\frac{d\sigma}{dq^2} = \frac{1}{2}\frac{G_F^2}{4\pi}\left[1 - \frac{q^2}{4E_\nu^2}\right][(1 - 4sin^2\theta_W)ZF_Z(q^2) - NF_N(q^2)]^2 \tag{6.68}$$

6.6.1 Differential cross section in terms of T

The differential cross-section in terms of T can be calculated as:

The three-momentum transfer is given by

$$q^2 = 2M_A T + T^2 \approx 2M_A T \tag{6.69}$$

$$\frac{dq^2}{dT} = 2M_A \tag{6.70}$$

By chain rule,

$$\frac{d\sigma}{dT} = 2M_A \left[\frac{d\sigma}{dq^2}\right] \tag{6.71}$$

$$\frac{d\sigma}{dT} = \frac{G_F^2 M_A}{4\pi}\left[1 - \frac{2M_A T}{4E_\nu^2}\right][(1 - 4sin^2\theta_W)ZF_Z(q^2) - NF_N(q^2)]^2 \tag{6.72}$$

6.6.2 Total cross section

In term of T, we can write the total cross section for coherent neutrino nucleus scattering as follows:

$$\sigma_{\nu A} = \int_0^{T_{\max}} \frac{d\sigma_{\nu A}}{dT}(T)\, dT \tag{6.73}$$

where T_{max} is determined as,

$$T_{max} = \frac{E_\nu}{1 + \frac{M_A}{2E_\nu}} \tag{6.74}$$

6.7 Form Factor $F(q^2)$

The form factor describes the spatial distribution of nucleons within the nucleus.A weak charge distribution is exhibited by the nucleus. At low energies, the wavelength of the Z boson is greater than the nucleus dimension. At the limit, the nucleus can be considered as a point particle. As the three momentum transfer q approaches 1/R, the nucleus' interior structure becomes crucial.

The weak form factor is defined as the Fourier transform of the nucleus's weak charge distribution, $\rho_w(\vec{r})$.

$$F(q) \equiv \frac{1}{Q_W} \int \rho_W(r) e^{i\vec{q}\cdot\vec{r}}\, d^3\vec{r} \tag{6.75}$$

where $q = (T, \vec{q})$ is the 4-momentum transfer

$$Q_W \equiv \int \rho_W(\vec{r})\, d^3\vec{r} \tag{6.76}$$

We will adopt a method in which the the form factors for neutron and proton are same.

$$F_N(q^2) = F_Z(q^2) \equiv F(q^2) \in [0, 1]. \tag{6.77}$$

Our calculations will be on the basis Helm form factor. The Helm model describes the nucleonic distribution as a convolution of a uniform density with radius R_0 (box or diffraction radius) and a Gaussian profile. The folding width (s) determines the surface thickness. The Helm form factor is provided by,

$$F(q^2) = \left[\frac{3}{qR_0}\right] J_1(qR_0) \exp\left[-\frac{1}{2}q^2 s^2\right] \tag{6.78}$$

where $J_1(x)$ is first order spherical Bessel function and it is given by,

$$J_1(x) = \frac{\sin(x)}{x^2} - \frac{\cos(x)}{x} \tag{6.79}$$

The Helm form factor requires a surface thickness of 0.9 fm. The nuclear dependency is determined by,

$$R_o^2 = R^2 - 5s^2 \tag{6.80}$$

where,

$$R = 1.2A^{1/3}\, fm \tag{6.81}$$

The plot for Form factor v/s T is given below:

From eqn(6.74) we can see that the maximum recoil energy is given by:

$$T_{max} = \frac{E_\nu}{1 + \frac{M_A}{2E_\nu}} \tag{6.82}$$

For Gallium experiment the neutrino energy is 751 keV. Then the maximum recoil energy is calculated as:

$$T_{max} = 0.0170\, keV \tag{6.83}$$

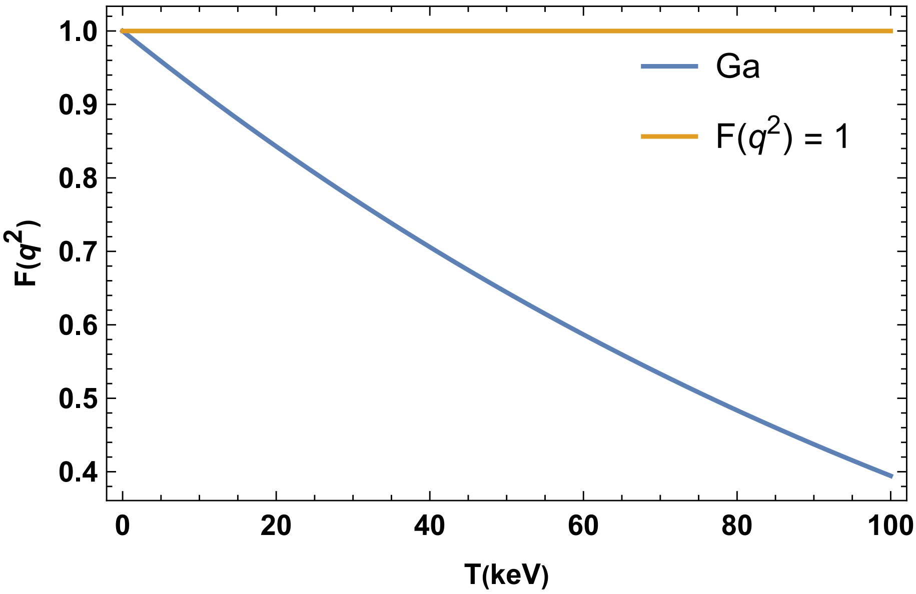

Figure 6.1: Form factor v/s T plot

As we can see from above graph that for low recoil energy the form factor can be taken approximately equal to 1. As in our case the maximum recoil energy is came out to be 0.0170 keV at which value the form factor can be taken as 1.

6.8 Differential Cross section

As we can see from the above plot for form factor that at low recoil energy the form factor:

$$F(q^2) \to 1 \tag{6.84}$$

Since the energy of recoil in our case is calculated as 0.0170 keV. For this value we can safely approximate the form factor $F(q^2) \approx 1$. Then the differential cross section is given by,

$$\frac{d\sigma}{dT} = \frac{G_F^2 M_A}{4\pi}\left[1 - \frac{2M_A T}{4E_\nu^2}\right][(1 - 4sin^2\theta_W)Z - N]^2 \tag{6.85}$$

6.9 Total Cross section

The total cross section for neutrino energy $E_\nu = 751\, keV$ can be calculated using equation(6.73):

$$\sigma_{\nu A} = \int_0^{T_{\max}} \frac{d\sigma_{\nu A}}{dT}(T)\, dT \tag{6.86}$$

Using eqn(6.73) and eqn(6.74), we can calculate this the net cross section. The net cross section at neutrino energy $E_\nu = 751\,keV$ is calculated as:

$$\sigma = 6.81 \times 10^{-41}\,cm^2 \tag{6.87}$$

We have approximated the form factor for the above calculation as $F(q^2) = 1$. However, we can take into account the form factor but it will not affect the result much. If we take into account the form factor and calculate the cross section we get:

$$\sigma = 4.35 \times 10^{-42}\,cm^2 \tag{6.88}$$

6.10 Conclusion

The cross section used for Charge current interaction neutrino-gallium reaction at neutrino energy $E_\nu = 751\,keV$ is

$$\sigma_{CC} = 5.39 \times 10^{-45}\,cm^2 \tag{6.89}$$

The cross section calculated for Coherent elastic neutral current channel is calculated as,

$$\sigma_{NC} = 4.35 \times 10^{-42}\,cm^2 \tag{6.90}$$

As we can see that the cross section calculated for CEvNS channel is three order of magnitude larger than the cross section for charged current channel. It means the CEvNS reaction is dominant in the neutrino gallium reaction. In gallium anomaly the ratio of measured to predicted event rate of germanium is:

$$R = 0.80 \pm 0.05 \tag{6.91}$$

From the value of the above ratio we can say the measured event rate is less than the predicted event rate. It means there could be the problem with the prediction of the event rate. It means in order to get the ratio equal to 1.

Our approach was to open the new channel of interaction, i.e neutral current channel. It could be possible that the few neutrinos are scattered by gallium nucleus via Coherent elastic neutral current interaction. As we can see from the above calculation, at the given energy of neutrinos, the cross section of CEvNS scattering is greater than the charge current interaction. It means we can not neglect the channel of elastic scattering in nucleus.

Bibliography

[1] V. N. Gavrin. Measurement of the solar neutrino capture rate in SAGE and the value of the pp-neutrino flux at the earth. *Nucl. Phys. B Proc. Suppl.*, 138:87–90, 2005.

[2] J. N. Abdurashitov, V. N. Gavrin, S. V. Girin, V. V. Gorbachev, T. V. Ibragimova, A. V. Kalikhov, N. G. Khairnasov, T. V. Knodel, V. N. Kornoukhov, I. N. Mirmov, A. A. Shikhin, E. P. Veretenkin, V. M. Vermul, V. E. Yants, G. T. Zatsepin, Yu. S. Khomyakov, A. V. Zvonarev, T. J. Bowles, J. S. Nico, W. A. Teasdale, D. L. Wark, M. L. Cherry, V. N. Karaulov, V. L. Levitin, V. I. Maev, P. I. Nazarenko, V. S. Shkol'nik, N. V. Skorikov, B. T. Cleveland, T. Daily, R. Davis, K. Lande, C. K. Lee, P. S. Wildenhain, S. R. Elliott, and J. F. Wilkerson. Measurement of the response of a gallium metal solar neutrino experiment to neutrinos from a ^{51}Cr source. *Phys. Rev. C*, 59:2246–2263, Apr 1999.

[3] J. N. Abdurashitov et al. Solar neutrino results from SAGE. *Phys. Atom. Nucl.*, 63:943–950, 2000.

[4] Aldo Ianni. Solar neutrinos. *Prog. Part. Nucl. Phys.*, 94:257–281, 2017.

[5] W. Hampel et al. Final results of the Cr-51 neutrino source experiments in GALLEX. *Phys. Lett. B*, 420:114–126, 1998.

[6] J. N. Abdurashitov, V. N. Gavrin, S. V. Girin, V. V. Gorbachev, P. P. Gurkina, T. V. Ibragimova, A. V. Kalikhov, N. G. Khairnasov, T. V. Knodel, V. A. Matveev, I. N. Mirmov, A. A. Shikhin, E. P. Veretenkin, V. M. Vermul, V. E. Yants, G. T. Zatsepin, T. J. Bowles, S. R. Elliott, W. A. Teasdale, B. T. Cleveland, W. C. Haxton, J. F. Wilkerson, J. S. Nico, A. Suzuki, K. Lande, Yu. S. Khomyakov, V. M. Poplavsky, V. V. Popov, O. V. Mishin,

A. N. Petrov, B. A. Vasiliev, S. A. Voronov, A. I. Karpenko, V. V. Maltsev, N. N. Oshkanov, A. M. Tuchkov, V. I. Barsanov, A. A. Janelidze, A. V. Korenkova, N. A. Kotelnikov, S. Yu. Markov, V. V. Selin, Z. N. Shakirov, A. A. Zamyatina, and S. B. Zlokazov. Measurement of the response of a ga solar neutrino experiment to neutrinos from a ^{37}Ar source. *Phys. Rev. C*, 73:045805, Apr 2006.

[7] Steven R. Elliott, Vladimir Gavrin, and Wick Haxton. The Gallium Anomaly. 6 2023.

[8] J. P. Kozlova, E. P. Veretenkin, V. N. Gavrin, A. I. Zvir, T. V. Ibragimova, and V. A. Tarasov. Measurement of Activity of an Artificial Neutrino Source in the Best Experiment by the Calorimetric Method. *Phys. Atom. Nucl.*, 83(6):958–961, 2020.

[9] V. N. Gavrin, T. V. Ibragimova, J. P. Kozlova, V. A. Tarasov, E. P. Veretenkin, and A. I. Zvir. Measurement of neutrino source activity in the experiment BEST by calorimetric method. *JINST*, 16(04):P04012, 2021.

[10] V. V. Barinov et al. Results from the Baksan Experiment on Sterile Transitions (BEST). *Phys. Rev. Lett.*, 128(23):232501, 2022.

[11] Vedran Brdar, Julia Gehrlein, and Joachim Kopp. Towards resolving the gallium anomaly. *JHEP*, 05:143, 2023.

[12] C. Giunti, Y. F. Li, C. A. Ternes, O. Tyagi, and Z. Xin. Gallium Anomaly: critical view from the global picture of ν_e and $\overline{\nu}_e$ disappearance. *JHEP*, 10:164, 2022.

[13] W. Hampel and L. P. Remsberg. Half-life of ^{71}Ge. *Phys. Rev. C*, 31:666–667, Feb 1985.

[14] S. M. Bilenky, C. Giunti, J. A. Grifols, and E. Masso. Absolute values of neutrino masses: Status and prospects. *Phys. Rept.*, 379:69–148, 2003.

[15] G. Garvey, E. Kolbe, K. Langanke, and S. Krewald. Role of strange quarks in quasielastic neutrino scattering. *Phys. Rev. C*, 48:1919–1925, 1993.

[16] F. J. Ernst, R. G. Sachs, and K. C. Wali. Electromagnetic form factors of the nucleon. *Phys. Rev.*, 119:1105–1114, 1960.

[17] A. Acha et al. Precision Measurements of the Nucleon Strange Form Factors at Q**2 ~ 0.1-GeV**2. *Phys. Rev. Lett.*, 98:032301, 2007.